CHAPTER - 1

INTRODUCTION

1.1 WHAT IS REMOTE SENSING?

Remote sensing is the science of acquiring information about the object or feature on the Earth surface without any physical contact. This can be done by scanning the Earth surfaces from a satellite or aircraft flying at high altitude. The remote sensing sensors captures the emitted or reflected radiation from the Earth surface features in different wavelength regions and records the data on a film or in a digital format. These data are used for the formation of images. The remote sensing images has the capability to provide useful information over vast area in a shorter time making it beneficial for the management of resources and accelerating national development.

There are various processes involved in acquiring information of the target on Earth surface using the remote sensing based approach as shown in Figure 1.1. Firstly, the source of energy or electromagnetic radiation is required for the illumination of the Earth surface targets. These radiation passes through the atmosphere where some part of radiation gets scattered, some gets absorbed and the rest gets transmitted and reaches the target on the Earth surface. This radiation interacts with the target where phenomena of absorption, transmission and reflection/emission takes place. This reflected or emitted electromagnetic radiation again travels through the atmosphere and reaches the satellite where this electromagnetic energy is captured and recorded by the sensor. This data is then transmitted to the antenna receiver at the ground stations in electronic form and processed in the form of a digital image. These

images obtained are further used for interpreting and anlayzing to extract the information about the Earth surface features.

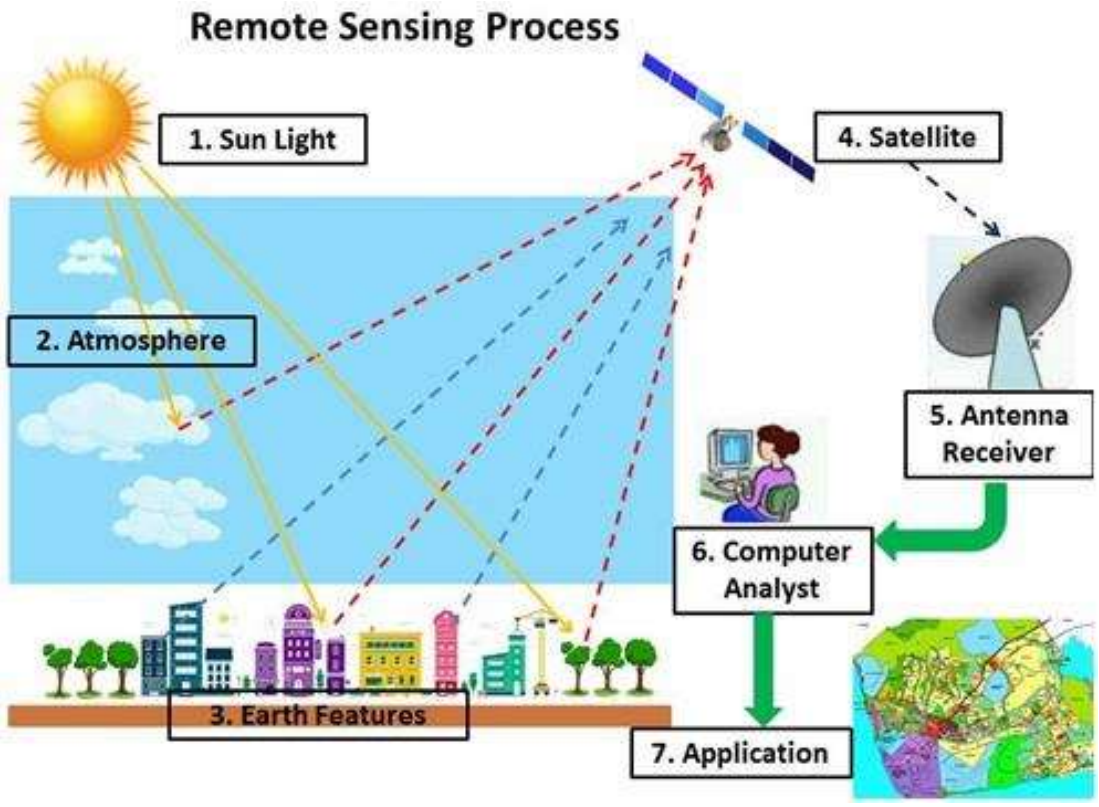

Figure 1.1 Remote sensing process

(**Source**:https://www.gisoutlook.com/2019/05/remote-sensing-introduction-termremote.html)

Remote sensing data can provide various informations about the atmosphere, waterbodies (like oceans, river) and land features. These data can be useful for various applications like agriculture, land-use land-cover (LULC) monitoring, environmental assessment, geology, geomorphology, hydrology, disaster management, urban planning etc.

1.2 TYPES OF REMOTE SENSING

Based on the source of energy required for illumination, remote sensing is categorized into two types i.e. passive remote sensing and active remote sensing. Both the remote sensing process is shown in Figure 1.2.

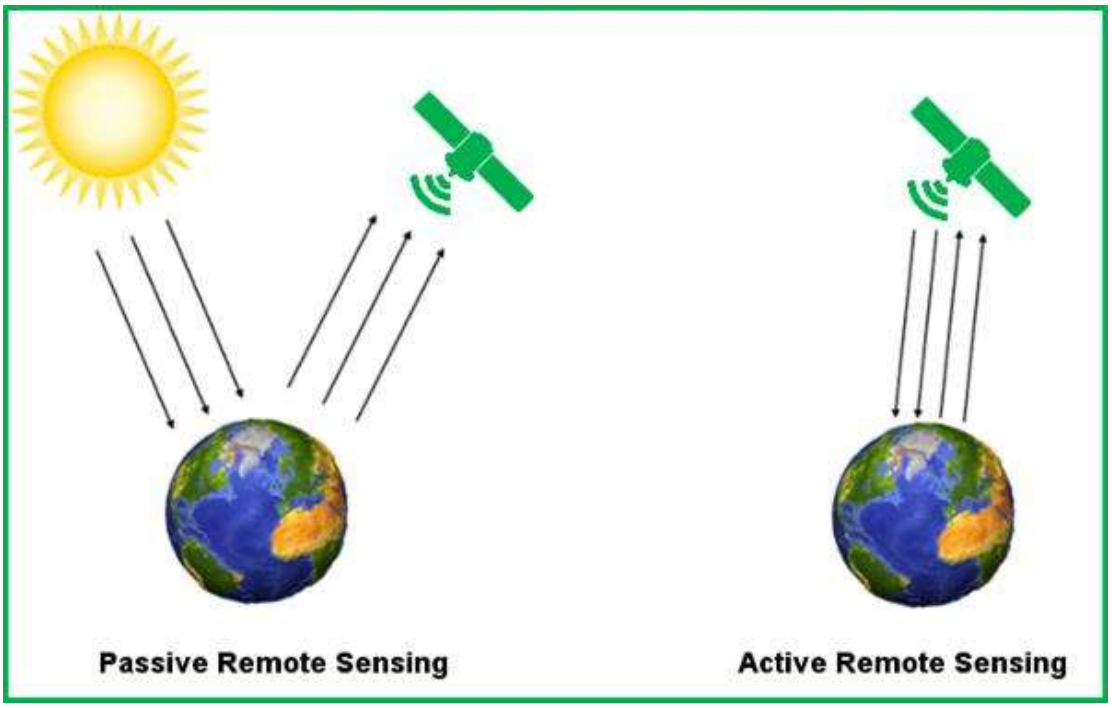

Figure 1.2 Passive and active remote sensing

(Source: https://grindgis.com/remote-sensing/active-and-passive-remote-sensing)

1.2.1 Passive remote sensing

Passive remote sensing is a remote sensing system where the source of energy used for illumination is naturally available. The sun is a natural source of electromagnetic radiation that is quite useful and convenient for various remote sensing systems. The electromagnetic radiation from the sun that reaches the Earths surface gets either reflected or emitted. The visible, near infra-red (NIR) and short-wave infra-red (SWIR) portions of the wavelength

gets reflected from the Earths surface. Thus, the NIR and SWIR portion of infra-red (IR) region is also referred to as reflected IR wavelengths. Some portions of mid IR region gets emitted from the Earths surface and is known as thermal IR wavelengths. The reflected energy is available only during day time when sun illuminates. Since, reflected energy is not available during night time, it is detected by passive sensors only during day time. The energy naturally emitted from the Earths surface (thermal IR wavelengths) can be detected both during day and night time. The energy detected by passive sensors is also sensitive to the weather condions. Most of the optical satellites uses passive sensors for detecting electromagnetic radiation from the Earths surface. Some examples are Land Remote-Sensing Satellite System (LANDSAT), The Advanced Spaceborne Thermal Emission and Reflection Radiometer (ASTER), Advanced Very High Resolution Radiometer (AVHRR), Moderate Resolution Imaging Spectroradiometer (MODIS), Quickbird, Rapid Eye etc.

1.2.2 Active remote sensing

Remote sensing system which provides their own source of electromagnetic radiation is known as active remote sensing. The energy is generated and transmitted from the sensor towards the target on Earths surface and the energy reflected or emitted by the target is detected and recorded by the sensors. Active sensors can be operational at all times irrespective of the season and time of the day. Measurements can be done both during day as well as night time. Active sensors are capable to work in those wavelength intervals that are not adequately provided by the naturally available source i.e. sun. However, the energy from active sensors must be generated in large amount such that adequate energy reaches the target of interest for illumination. Microwave remote sensing uses active sensors as sun cannot provide sufficient energy for illumination in the wavelengths of microwave region. Some examples of active sensors are Radio Detection And Ranging (RADAR), Light Detection and

Ranging (LIDAR), Sound Navigation Ranging (SONAR), Synthetic Aperture Radar (SAR) etc.

1.3 THE ELECTROMAGNETIC SPECTRUM

The electromagnetic spectrum ranges from the gamma rays and X-rays having shorter wavelengths to that of microwave and radiowaves having longer wavelengths as shown in Figure 1.3. Several portions of this electromagnetic spectrum are useful for the purpose of remote sensing. Ultra-violet portion of the elctromagnetic spectrum (ranging from 0.1 μm to 0.4 μm) is the shortest wavelength useful for remote sensing. Some of the Earth surface features like rocks and minerals emits energy in the visible portion (ranging from 0.4 μm to 0.7 μm) when illuminated by UV light. The visible portion of the electromagnetic spectrum can only be detected by human eye. Various sensors have been developed that has the capability to detect the other parts of the spectrum that cannot be detected by human eye. The next segment of the electromagnetic spectrum is the IR spectrum whose wavelength ranges from 0.7 μm to 100 μm. This spectrum can be further divided into two segments based on their properties of interaction with the Earth targets i.e. reflected IR and thermal IR. The reflected IR lies in the wavelength range of 0.7 μm to 3 μm and the thermal IR lies in the wavelength range of 0.3 μm to 100 μm. The visible and the reflected IR region in the electromagnetic spectrum is used for remote sensing in a similar manner but the thermal IR wavelength of the spectrum is quite different. The energy that is emitted from the Earths surface in the form of heat lies in the thermal IR wavelength part of the spectrum. The microwave region are the longest wavelengths that are useful for the remote sensing purpose. The microwave part of the spectrum lies in the wavelength range from 1 mm to 1 m.

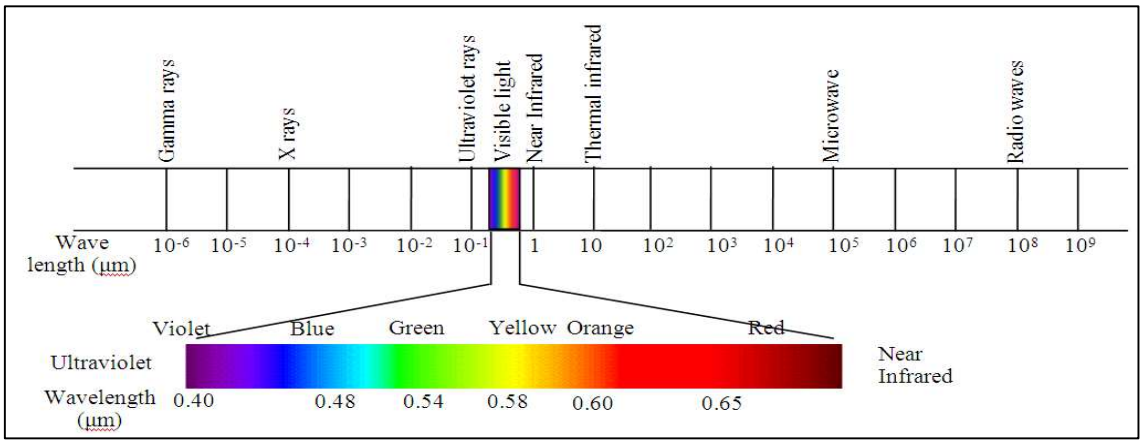

Figure 1.3 The electromagnetic spectrum

(Source: semanticscholar.org)

1.4 INTERACTION OF EMR WITH ATMOSPHERE

The electromagnetic radiation from the source travels through the atmosphere before reaching the Earths surface. The atmosphere comprises of particles and gases which can effect the incoming radiation by the phenomena of scattering and absorption.

1.4.1 Scattering

Scattering takes place when the incoming electromagnetic radiation interacts with the gases and molecules present in the atmosphere. This scattering phenomena mainly depends on the factors i.e. the wavelength of incident radiation, the density of the particles, molecules or gases present in the atmosphere and the distance that radiation travels through the atmosphere.

The scattering phenomena has been categorized into three types i.e. Rayleigh scattering, Mie Scattering and Non-selective scattering. The phenomena of Rayleigh scattering occurs when the size of the particles present in the atmosphere are very small in comparison to the wavelength of the incident radiation. These particles may include small

flecks of dust and nitrogen or oxygen molecules in the atmosphere. This scattering mechanism results in dominant scattering of shorter wavelengths than the longer wavelengths and is more dominant in the upper atmosphere. The phenomena of Mie scattering occurs when the size of the particles present in the atmosphere are equivalent to the wavelength of the incident radiation. This scattering mechanism occurs in the lower part of the atmosphere due to the presence of the dust, smoke, pollen and water vapour and affects the longer wavelengths as compared to those scattered by Rayleigh scattering. The phenomena of non-selective scattering ocurs when the size of particles present in the atmosphere are quite large as compared to the wavelength of incident radiation. This type of scattering is caused by large dust particles and water droplets which scatters all the wavelengths almost equally.

1.4.2 Absorption

Absorption can be defined as a process in which some part of the incident energy from the electromagnetic radiation gets absorbed by the particles present in the atmosphere at different wavelength ranges. The gaseous components in the atmosphere absorbs the incident electromagnetic energy at selective wavelength regions that depends on their energy levels and the distribution of the atmospheric constituents. Thus, the electromagnetic radiation from the Sun containing all the wavelengths travels through the atmosphere where some part gets absorbed allowing only specific wavelengths of electromagnetic radiation to pass through the atmosphere and reach the Earths surface. The wavelength ranges of the electromagnetic spectrum that are transparent to the atmosphere is known as atmospheric windows. These wavelengths are useful for remote sensing purpose and are shown in Figure 1.4. The wavelength regions shorter than 0.3 μm are mostly absorbed by the ozone (O_3). The atmosphere allows the passage of visible part of the spectrum and can be considered as transparent to the atmosphere. The wavelength bands in the IR portion of the spectrum are

mainly absorbed by the carbon-dioxide (CO_2) and water vapour (H_2O) molecules. The most part of the far IR portion of spectrum is absorbed by the atmosphere. The microwave regions is almost completely transparent to the atmosphere.

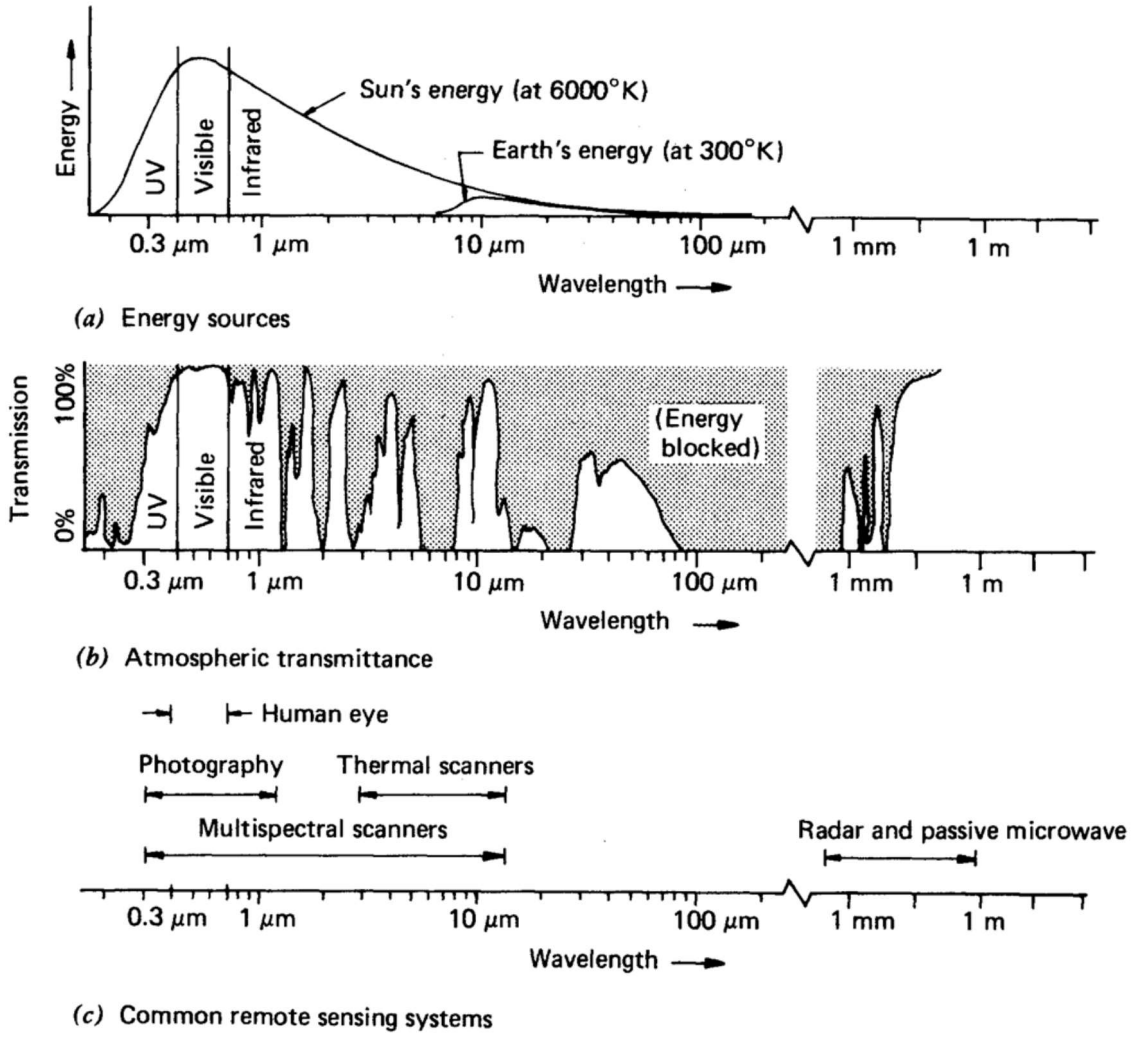

Figure 1.4 The electromagnetic spectrum useful for remote sensing

(Source: Lillesand et al., 2004)

The reflected IR and the visible portion of the radiation in the atmospheric window is useful for the optical remote sensing. The wavelength, ranging from 3 to 14 μm, has been

considered for thermal remote sensing because Earth emits energy in this range of electromagnetic spectrum. Atmospheric absorption is significant in the wavelength range of 5 to 8 µm. There are two narrow windows in the thermal IR portion i.e. 3 to 5 µm and 8 to 14 µm. The sun emits energy in the UV, visible and IR portion of the spectrum. Thus, sun acts a souce of illumination for optical and thermal remote sensing.

1.5 INTERACTION OF EMR WITH THE EARTH SURFACE FEATURES

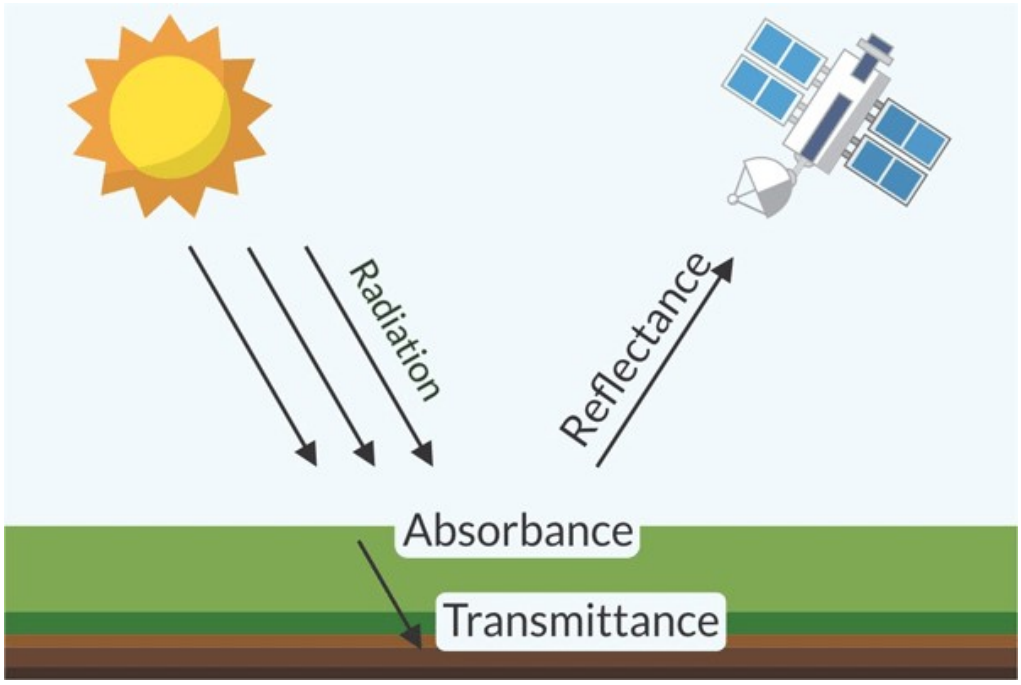

Figure 1.5 Interaction of radiation with the Earth surface features

(**Source**: https://webapp.agron.ksu.edu)

The part of electromagnetic radiation that neither gets scattered nor absorbed by the atmosphere reaches the Earths surface and this radiation interacts with the land target features. The interaction of incident radiation with the Earth surface features occurs in three

different ways i.e. absorption (A), transmission (T) and reflection (R) as shown in Figure 1.5. Absorption occurs when some part of the incident radiation is absorbed by the land targets. Transmission occurs when some part of incident radiation passes through the land target. Reflection occurs when incident radiation bounces off the target and its path gets redirected.

The reflected energy is useful for remote sensing as it contains information about the land target features. There are two types of reflection based on the direction of reflected energy from the target i.e. specular and diffuse reflection. The surface roughness and the wavelength of the incident radiation determines the type of reflection that may occur from a surface. When the surface roughness is less than the incident wavelength, then the surface is considered as smooth surface resulting in specular reflection whereas when the surface roughness is greater than the incident wavelength, then the surface is considered as rough surface resulting in diffuse reflection. Most of the Earth surface features shows partly specular and partly diffuse reflection.

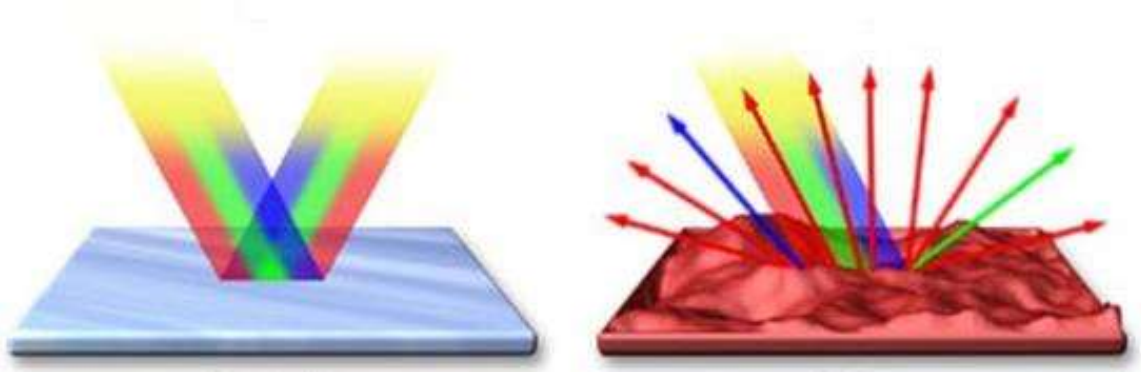

(a) (b)

Figure 1.6 Types of reflection (a) Specular reflection and (b) Diffuse reflection

(**Source**: https://micro.magnet.fsu.edu/)

1.5.1 Spectral reflectance

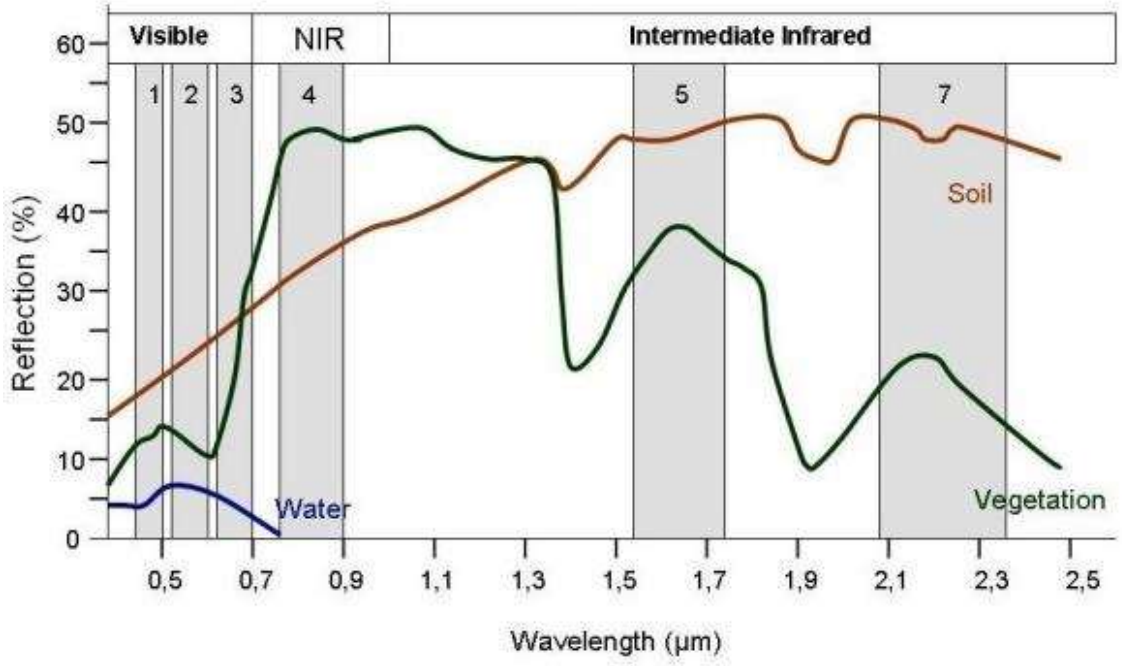

Figure 1.7 Spectral reflectance curve of water, soil and vegetation

(**Source**: : https://arset.gsfc.nasa.gov)

The ratio of energy reflected from a target feature on Earth surface to that of the energy incident at a particular wavelength is defined as the spectral reflectance of that target feature. This spectral response helps in identification of the target on the Earth surface. The graphical respresentation of the spectral reflectance values of the Earth surface feature over different wavelengths of the electromagnetic spectrum is known as spectral reflectance curve. Figure 1.7 shows the spectral reflectance curve of three major land covers i.e. vegetation water and soil. Water shows some reflectance value in the visible region of spectrum and negligible in IR part of spectrum. Water absorbs all the incoming IR radiation. Vegetation shows higher reflectance value in the NIR region whereas very low reflectance is observed at

red and blue wavelengths in the the visible region.This spectral response of vegetation depends upon the properties of the leaves i.e. chlorophyll content, cell structure, the distribution and arrangement of leaves in an area. The dry soil shows higher reflectance values in the SWIR region and lower in the visible region of spectrum. The reflectance value in IR region drops for the case of wet soil due to the presence of moisture content in the soil.

1.6 DIGITAL IMAGE REPRESENTATION

The electromagnetic energy coming from the Earths surface can be recorded in photographic or electronic form. The electronic form of image representation is a digital image. A digital image can be sub-divided into small picture elements or pixels. Pixel refers to a smallest unit of a digital image which has equal size and shape in the image. Pixel size is considered as the size of the smallest feature that can be detected from a digital image. The brightness value of each pixel is represented with numeric value named as digital number (DN). The distribution of pixels and the DN values representation is shown in Figure 1.8. It is shown that the pixels that appear brighter in the digital image is provided with a larger DN values whereas the pixels appearing darker in the image is provided with lower DN values

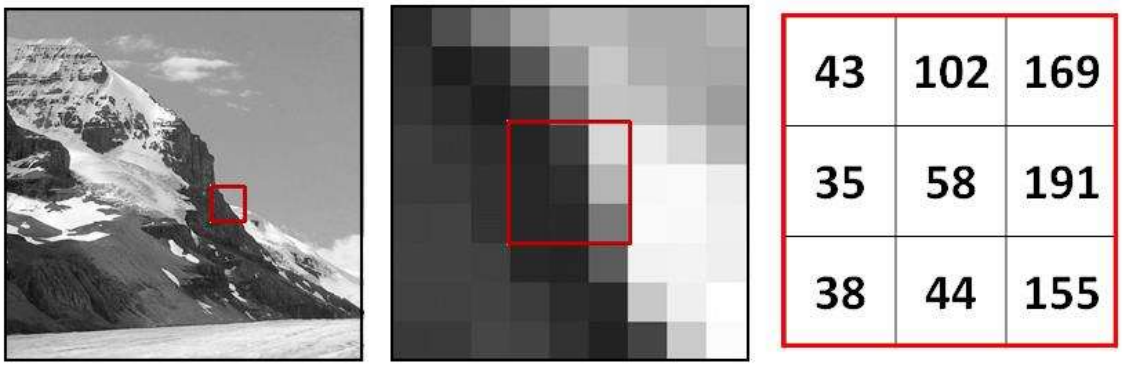

Figure 1.8 Digital image representation

(Source: https://gsp.humboldt.edu/)

1.7 SATELLITE CHARACTERISTICS

The satellite follows a fixed path in the space known as orbits. The satellite orbits are categorized based on the objective and the capability of the sensor into two types i.e. equatorial and polar orbit as shown in Figure 1.9. The satellite, kept at a very high altitude (almost 36000 km) in the equatorial plane, appears stationary to the observer on the Earth surface is known as geostationary or equatorial orbit. The geostationary satellite revolves at a speed that matches the Earth's rotation. This helps in continuous tracking and collecting information over a fixed location. Weather and communication satellites are mainly placed at equatorial orbit and it has the capacity to observe a very large area on the Earth surface (sometimes entire hemisphere of Earth) due to its higher altitude. The satellites that moves from north to south, inclined at an angle ~90^0 and placed at an altitude of approximately 800 km, have polar orbits. It has capability to make more than one revolution in a day. The Earth's rotation from West to East makes the satellite to pass over different areas in each revolution. This enables the polar satellite sensor to acquire information of the entire Earth surface. Most of the polar orbits are also sun-synchronous as they cover each area on Earth surface at a fixed local time of the day named as local sun time. These satellites are mainly used for Earth observation and provides more detailed image due to their lower altitude as compared to equatorial orbit.

The sensor onboard satellite views a certain area on the Earth surface at a particular time. The width of the area on the Earths surface imaged by the sensor when the satellite passes above a region is known as swath.

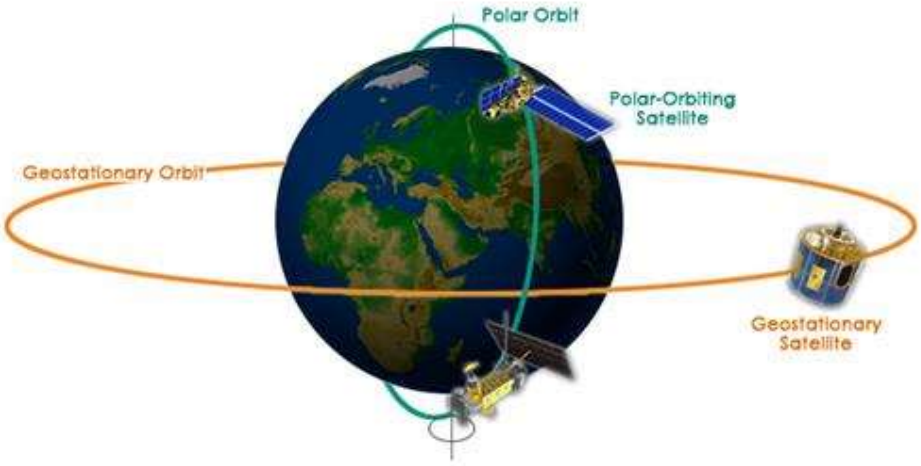

Figure 1.9 Equatorial and Polar orbit

(**Source**: www.open.edu/openlearn/ocw/mod/oucontent/view.php?id=77544&section=5)

1.8 CHARACTERISTICS OF REMOTE SENSING IMAGE

The quality of a remote sensing image depends on the sensor properties and the distance of the target on Earth's surface from the satellite platform. There are four types of resolution responsible for the quality of image i.e. spatial, spectral, radiometric and temporal resolution.

1.8.1 Spatial resolution

The size of the smallest dimension of the target on Earth surface detected by the sensor is referred to as the spatial resolution of the image. All the objects on Earth surface having dimension greater than that of the spatial resolution of a particular sensor can be detected by that sensor. The spatial resolution of an image primarily depends two factors i.e. the Instantaneous Field of View (IFOV) and the altitude of the satellite platform that contains sensor from the Earth surface. The solid angle through which a sensor can detect the

electromagnetic radiation from the Earth surface is known as IFOV. The multiplication of the IFOV and the altitude of sensor determines the area on the Earth surface as seen by the sensor at a particular moment of time. The Figure 1.10 shows three false colour composite (fcc) images of the same location at three different spatial resolutions of 500 m, 30 m and 10 m. The image with 500 m, 30 m and 10 m spatial resolution were obtained from MODIS, Landsat and Sentinel-2 data, respectively. It can be observed that the smaller features can be identified in the image with 10 m and 30 m resolutions as compared to that of 500 m resolution image.

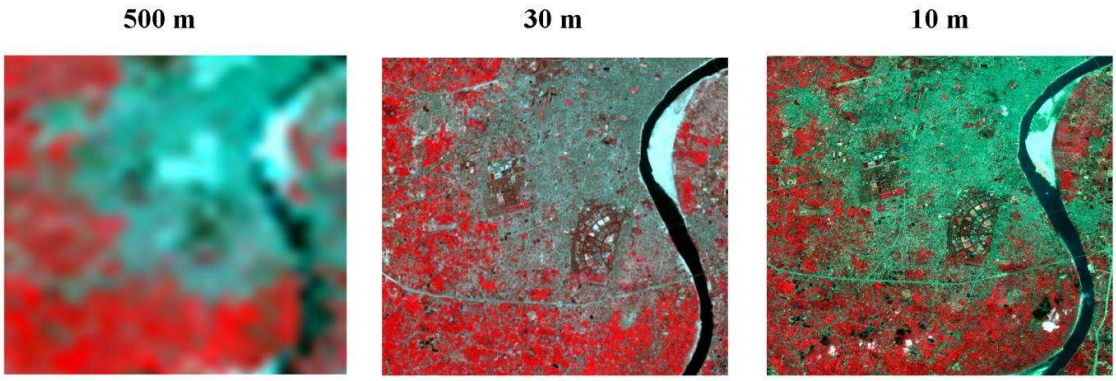

Figure 1.10 Images of same location of Varanasi city at a spatial resolution of 500 m, 30 m and 10 m

1.8.2 Spectral resolution

The spectral resolution refers to the ability of a sensor to use finer wavelength intervals for making remote sensing observation. Various remote sensing sensors records energy at different wavelength intervals from different features on the Earth surface for their identification by interpretation of the spectral response at different wavelength ranges. The Figure 1.11 shows that a black and white film records the combined reflectance in the wavelength range of 0.4 to 0.7 μm whereas a colour film provides reflectance values at three

different wavelength range i.e. 0.4-0.5 µm, 0.5-0.6 µm and 0.6-0.7 µm. So, the black and white film has coarser spectral resolution whereas the colour film has finer spectral resolution. More features can be distinguished from an image through a colour film as compared to that from a black and white film.

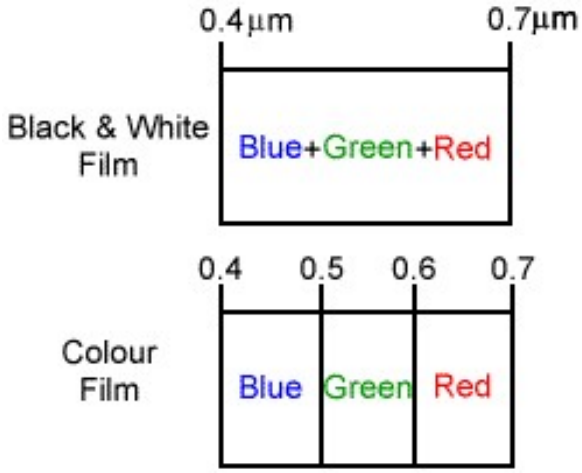

Figure 1.11 Spectral resolution

(**Source**: http://gsp.humboldt.edu)

The broad wavelength intervals can be useful for distinguishing broad land cover classes like vegetation, soil, water etc. which is possible when using multispectral sensors. The comparison of the energy recorded at finer wavelength intervals is required to distinguish more fine details about the features like types of rocks and vegetation, vegetation health, water quality etc. The hyperspectral sensors provide reflectance at very fine wavelength intervals. The hyperspectral data may provide almost 200 bands with a narrow bandwidth of 5 to 10 nm whereas the multispectral data provides 3 to 10 bands with a broader bandwidth of 70 to 400 nm in the wavelength region of visible and IR spectrum.

1.8.3 Radiometric resolution

The radiometric resolution can be defined as the potential of the sensor to discriminate small differences in electromagnetic energy reaching the sensor from the Earths surface. The sensor that provides digital image at finer radiometric resolution is more sensitive to distinguish between the fine differences in energy of the reflected or emitted radiation. The DN value of an image varies from 0 to 2^n -1. Here, n is the number of bits. The number of bits of an image represents the radiometric resolution. Figure 1.12 shows three images at a radiometric resolution of 8 bits, 2 bits and 1 bit. The 8 bits image shows more detailed difference in the reflected or emiited energy as compared to those images with a radiometric resolution of 2 bits and 1 bit. This is due to the availability of 256 brightness levels in 8 bit image, 4 brightness levels in 2 bit image and 2 brightness levels in 1 bit image to represent an image.

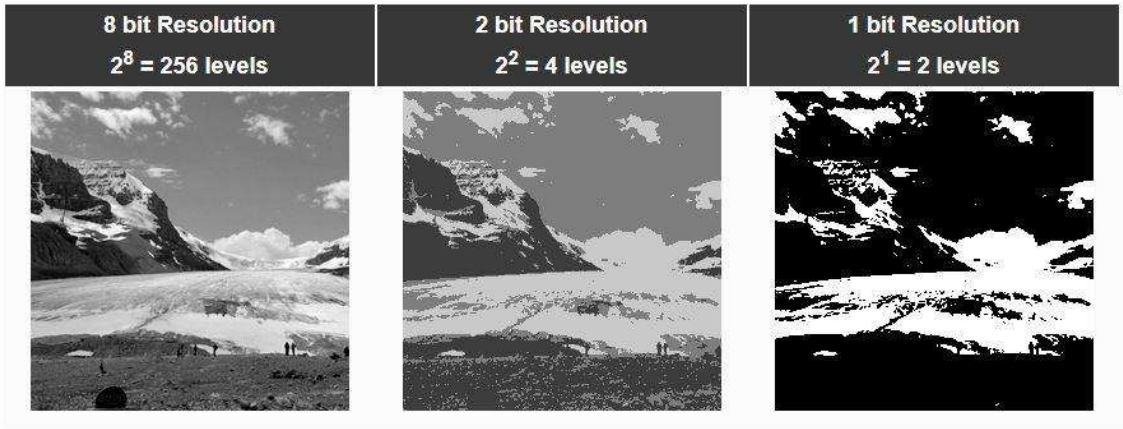

Figure 1.12 Images of same location at a radiometric resolutions of 8, 2 and 1 bits

(**Source**: http://gsp.humboldt.edu)

1.8.4 Temporal resolution

The temporal resolution refers to the length of time required by the satellite sensors to revisit and collect data of exactly the same position on the Earth surface. The spectral characteristics of the features on Earth surface at a particular location may change with time. The multitemporal imagery helps us to study about the changes occurred on the Earths surface at the same location in a specific time interval. The multitemporal images can be useful for various applications like monitoring the crop growth in a season, urbanisation, effects of natural disasters (floods, earthquake, forest fire) and many more.

1.9 THERMAL REMOTE SENSING

Thermal remote sensing can be defined as the remote sensing process in which the sensor senses the energy emitted from the Earths surface in the thermal infra-red (TIR) region of the electromagnetic spectrum having wavelengths in the range of 3 to 15 μm. The radiation in the wavelength range 5 to 8 μm are strongly absorbed by the atmospheric constituents. Thus, only two bands i.e. 3 to 5 μm and 8 to 14 μm are used for thermal remote sensing. Various multispectral scanning systems (MSS) senses energy in the visible, reflected IR and TIR wavelength bands. Optical remote sensing detects the reflected wavelengths whereas the thermal remote sensing detects emitted radiation from the Earths surface. This makes the thermal remote sensing complementary to that of optical remote sensing. Thermal sensors consisting of photo-detectors are sensitive to the photons. They have capability to detect the thermal radiation emitted from the Earths surface. The information acquired by the thermal sensors about the emitted thermal radiation are useful for measuring the thermal properties of the target material and the surface temperatures. The longer wavelength of TIR band as compared to the visible and reflected IR band results in minimal atmospheric scattering. The energy is inversely proportional to the wavelength as shown in Equation 1.1.

$$E = \frac{hc}{\lambda} \quad (1.1)$$

Where, h is the Plancks constant with value of 6.626×10^{-34} J.s, c is the speed of light with value 3×10^{8} m/s and λ is the wavelength of the radiation. The energy of wavelengths in TIR band is lower than the energy of visible and reflected IR wavelengths. In order to ensure that sufficient amount of energy emitted from the Earths surface in thermal regions reaches the sensor, larger IFOV is required for a reliable measurement. Thus, the spatial resolution of thermal bands obtained from a satellite sensor are coarser as compared to that of visible and reflected IR bands.

A basic knowledge of thermal radiation is required for the analysis of the thermal images acquired by the sensors. All the objects with temperature above 0 K emits electromagnetic radiation. The electromagnetic energy emitted from the target materials can be related to temperature as given by Wien's displacement law and Stefan-Boltzmann law. According to Stefan-Boltzmann law, the total energy emitted by a blackbody is related to temperature as shown in Equation 1.2.

$$M = \sigma T^4 \quad (1.2)$$

Where, M = total energy emitted from a materials surface in W m^{-2}, σ = Stefan-Boltzmann constant having a value of 5.6697×10^{-8} W m^{-2} K^{-4} and T = absolute temperature of the material emitting radiation in unit of K. According to Wien's law, the wavelength at which the blackbody emits maximum energy is related to temperature as shown in Equation 1.3.

$$\lambda_m = \frac{2898}{T} \quad (1.3)$$

Where, λ_m = dominant wavelength in μm and T = temperature in K. Both the laws are applicable for a perfect blackbody having emissivity value of 1. However, the natural

materials are not perfect blackbodies as their emissivity value ranges from 0 to 1. Thus, the temperature obtained from TIR radiation using the blackbody laws i.e. Wien's and Stefan-Boltzmann law is less than the actual or true surface temperature. The ratio of the energy radiated from the natural surface to that radiated from a blackbody at the same temperature and wavelength is defined as emissivity. A blackbody shows emissivity value of 1 and considered as a perfect emitter. The target materials with higher emissivity value absorbs and emit comparably higher proportions of incident electromagnetic energy. The true surface temperature of a material can be determined by incorporating the approximate emissivity values in the blackbody radiation law. The Earth emits energy at 300 K with dominant wavelength of 9.7 μm. The thermal sensors can detect the thermal radiation from the Earths surface at all times of the day and night.

Researchers have used various methods for the retrieval of Land surface temperatures (LST) from different satellite data like Single Channel Algorithm, Split Window Algorithm, Multi-channel Algorithm, Radiative Transfer equation based method etc. It was found that LST could be retrieved with reasonable accuracy (Jiménez-Muñoz et al. 2010; Tsou et al. 2017; Wan et al. 2002; Mallick et al. 2008; Coll et al. 2005; Yu et al. 2014). Thermal bands in a satellite data are most important for determination of LST. Emissivity and other atmospheric parameters like upwelling radiance, downwelling radiance, transmissivity etc. are also required to remove the atmospheric effects for estimation of LST. Various satellites contain thermal bands like Landsat, Aster, AVHRR, MODIS. The urban areas shows greater heterogeneity in land covers. The study on LST variation in urban regions require finer spatial resolution thermal images. Landsat and Aster data are widely used for LST retrieval in urban areas due to their finer spatial resolution of thermal bands to study the spatial variation in LST with different urban landscapes.

1.10 APPLICATIONS OF THERMAL REMOTE SENSING

Thermal remote sensing senses the emitted radiation from the Earths surface which represents the thermal property of a material. This helps in identification of surface materials, rock types, soil moisture etc. The ability to detect minor temperature variations can be useful to extend our observation on various phenomena to understand our environment. The following list provides some areas where thermal data is used.

- Surface temperature detection
- Seismology
- Urban heat island analysis
- Oil spill monitoring
- Soil moisture estimation
- Water quality monitoring
- Drought monitoring
- Evapotranpiration monitoring
- Forest fire detection
- Volcanic activity monitoring
- Coal fires
- Environmental modelling

1.11 SURFACE URBAN HEAT ISLANDS

The Surface Urban Heat Island (SUHI) refers to the urban areas whose surface and atmospheric temperatures are significantly higher than the surrounding rural areas due to urbanization, especially during night time. Urbanization has resulted in replacement of larger areas consisting of natural land surfaces with that of man-made artificial built-up surfaces (Voogt and Oke 2003; Oke, 1987). The built-up surfaces are made up of non-evaporating

impervious materials. The urban materials are made of asphalt, concrete, construction material. These materials absorbs greater heat from the sun and then releases energy resulting in higher urban temperatures. SUHIs are formed due to the increase in artificial materials that have high heat capacities, increase in anthropogenic heat discharge by industries, vehicles, buildings and also decrease in vegetation and natural pervious surfaces that reduces temperatures through evapotranspiration. Compact urban geometry also contributes to temperature rise due to less convection. The phenomena of SUHI effect has been observed, recorded and studied for more than 150 years (Howard, 1833). The dynamics of SUHI effect depends on various factors i.e. time, local and urban feature characteristics, metereological conditions which reveals its uniqueness for different urban areas.

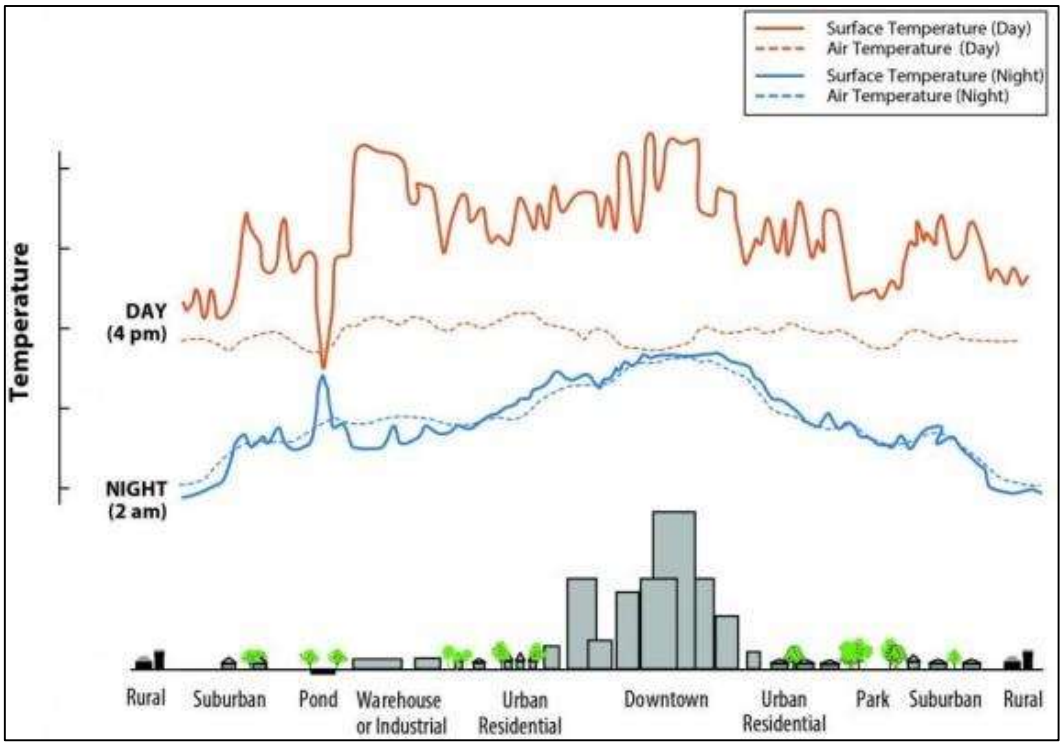

Figure 1.13 Surface urban heat islands

(**Source**: www. pa.gov/sites/production/files/2020-07/documents/heat-island-webcast-equity-2020-06-03.pdf)

The development and expansion of cities without proper planning gives rise to various harmful air pollutants from industries, power plants and exhaust emissions from vehicles. These air pollutants has the tendency to absorb solar radiation and hence, contributes in raising temperature. People from rural areas have been migrating to the urban areas due to availability of various facilities like hospitals, schools, transports etc. that has increased human gathering in urban areas. This gives rise to greater emission of carbon dioxide which absorbs heat and increases the atmospheric temperature contributing to the SUHI. Vegetation losses in urban areas cause loss of shade and cooling effect from trees and also increase in carbon dioxide. Urban areas have mutilayer buildings and hence the heat reflected by a building is absorbed by other nearby tall buildings giving rise to urban canopy. Greater amount of built-up areas reduces the wind velocity. Hence, heat is trapped in urban areas due to less convection. SUHI provides positive as well as negative effect. In summer season, this creates discomfort to people due to heat stress. Consequently, the demand for energy to cool buildings increases leading to increase the generation of power. This results to greater amount of greenhouse gas emission i.e. SO_2, NO_2, CO and CO_2 contributing to global warming and decline of the climate. However, in the winter season, rise in temperature provides comfort to the people.

Traditionally, SUHI effects were observed from the air temperature data observed from the fixed weather stations and airborne sensors. Then, the spaceborne sensors were developed which provides surface temperature data used for various applications by determining the relation of SUHI effect with urban climate. Rao (1972) first studied SUHI effect from the satellite sensor measurement. The presence of vegetation in abundance within urban environment controls temperature and air quality (Nowak et al. 2000).

1.12 IMPORTANCE OF LAND SURFACE TEMPERATURES ANALYSIS IN URBAN AREAS

The demand for air conditioners has increased due to the raising temperatures in the urban areas. The usage of air conditioners also degrades the environment due to the fog formation which increases the amount of pollutants in the atmosphere (Rosenfeld et al. 1995). Thus, higher urban temperatures has significant negative impact on our environment like rise in the pollution levels, increases in dryness and also modifies the natural precipitation cycle (Kato, 2005). As a result, the study of LST in urban areas with different pattern, magnitude and land covers has become important for the urban sustainable planning and environmental protection (Kaufmann, 2007; Grimm, 2008; Mountrakis, 2011; Md. Nuruzzaman, 2015). The net rise in temperature in urban areas depends on various factors that should be identified for the attenuation of SUHI effect. Simply comparing the urban temperatures to the surrounding rural temperatures is not an adequate method for analysing SUHI effect. Because, the rise in temperature associated with the SUHI effect is due to the complex interaction of electromagnetic radiation with the various land cover features.

1.13 RESEARCH QUESTIONS

According to the research work being carried out in the field of LST behaviour of different land covers in urban areas and effect of urbanisation on SUHI effect, some research questions have to be answered as mentioned below:

1. How can the LST images obtained from satellite sensor at coarse spatial resolution be disaggregated to obtain LST image at finer spatial resolution in heterogeneous urban areas?
2. How does the behaviour of LST change for different land covers during both day as well as night time?

3. How does the relationship of day and night LST varies with different spectral indices (SI) which represents abundance of a particular type of land cover?
4. How to quantify the intensity of SUHI effect with the change in land covers over urban landscapes and also determine contribution of each land cover towards SUHI effect?
5. How to quantify Surface urban heat island (SUHI) intensity with increased urbanisation and its variation with different seasons?

1.14 REVIEW OF LITERATURE

Zhang et al. 2010 studied the relationship between vegetation greenness and SUHI effect in Beijing, China using Landsat Thematic Mapper (TM) images. The Normalized Difference Vegetation Index (NDVI) and brightness temperature (T_b) were calculated and the spatial correlation was established between T_b and NDVI. It was found that T_b shows clear negative correlation with NDVI. The 66 feature profiles in NE-SW direction and 45 in NW-SE direction were selected and studied the relation of T_b with NDVI for each profile and found that the degree of correlation decreased from the centre of the urban area to the edge. Hence, greater complexity in land structures lead to greater correlation between T_b and NDVI. Manteghi et al. 2015 analysed the influence of water bodies on the urban temperatures. The temperature of water body was found lower than the neighbouring urban land covers by 2 – 6 ºC due to its high heat absorption capacity. Hence, the presence of waterbody can lead to evaporative cooling which might be an efficient system of passive cooling for urban environment during day time. However, at night time, water bodies maintain water temperatures due to its thermal inertia and high heat capacity. Hence, provides warming influence at night. Rinner and Hussain (2011) studied the relation of LST with different LULC of Toronto using Landsat TM data. The urban region includes the roads and parking lots, building roofs and walls, resource/industrial and commercial areas and also the parks

and recreation centres. They classified the image into these classes of built up areas and also acquired the thermal image of Toronto. On comparing the classified and LST images, the resource/industrial area and the commercial land uses were found to show higher temperatures (29.1ºC) due to high proportion of built up surfaces made up of low albedo materials having high heat capacity. The parks or recreation land (25.1ºC) and water bodies (23.1ºC) showed much lower LST values. Residential, open area land and the government/institutional land showed similar averaged temperature of 27.4 °C. These areas had averaged temperatures because they have vegetation such as lawns or trees occurring around built structures. Zhou et al. 2015 studied the diurnal and seasonal variation in SUHI effect in 32 cities of China using MODIS and Landsat TM and ETM+ images and found that SUHI was more prominent during night time and summer season. The LST value decreased exponentially with distance from the centre of the city to outside. SUHI footprint was observed larger during night time. Rasul et al. 2016 analyzed the diurnal and seasonal changes in Surface Urban Cool Islands (SUCI) and SUHI in Erbil, Iraq situated in the semi-arid climate using MODIS Terra/ Aqua images. From the MODIS LST maps, the dense built-up land covers experiences lower LST values in comparison to the non-urbanised area around the city during the daytime which results in SUCI effect. The city showed higher LST values during night time as compared to the neighbouring regions resulting in significant SUHI effect. The seasonal variation in the SUCI and SUHI effect was studied which showed that SUHI effect was stronger during night time of spring and summer season than the autumn and winter season. Daytime SUCI intensity was found to be higher in the autumn and summer than in winter and turned almost neutral in the spring. They also studied the relation of LST with NDVI at different seasons and found that LST shows negative relation with NDVI at all seasons except in winter. Luo and Li (2014) studied the effect of NDVI, Normalized Difference Built-up Index (NDBI) and Normalized Difference Water Index

(NDWI) on LST using Landsat TM images of Chongqing, China on 23 May 2010. Strong Heat Island centers were found at densely populated areas consuming high energy. The center of the city did not show significant SUHI effect due to the influence of river. The regression models were built to understand the relation of LST with the SI i.e. NDVI, NDBI and NDWI at different spatial scales. NDVI and NDWI showed negatively correlated whereas NDBI showed positively correlated and this correlation was found to increase with increasing spatial scales. Shastri et al. 2017 studied the SUHI effect during day time and night time of summer and winter season of 82 cities in India using MODIS data. The LST maps revealed negative SUHI effect in many cities of central and western part of India during day time whereas positive SUHI during night time of summer season. However, almost all cities showed positive SUHI effect during both day and night time of winter seasons. Due to low vegetation in rural areas, barren land showed very high LST resulting in negative SUHI during summer daytime. Summer mean night time SUHI and winter mean night time SUHI of different cities was found to be positively correlated with population and this correlation was greater for winter season. Sanjeewani and Manawadu (2016) studied the spatial trends of LST variation of four cities in Sri Lanka using Landsat 5 TM, Landsat 7 ETM+ and Landsat 8 Operational Land Imager (OLI) images from 1988 to 2015. LST was found to increase in central area of the cities due to higher built up region. LST also increased with high population density and road network. Mathew et al. 2015 studied the SUHI effect on Ahmedabad City using MODIS and Landsat 5 TM data. NDVI and NDBI obtained from Landsat 5 TM data was aggregated to 1 km spatial resolution for comparing it with MODIS night LST data. Higher LST values were shown by urban areas and LST pattern was found to be well distributed in the high density commercial, residential and industrial areas indicating SUHI effect. The LST showed negative correlation with both NDVI and Enhanced Vegetation Index (EVI) which interprets that the vegetated regions has the capability to

reduce the SUHI effect. Amiri et al. 2009 studied the temporal dynamics of LST and LULC types using Landsat 4,5 TM and Landsat 7 ETM+ sensors for different years. The temporal variability of thermal data and vegetated cover was investigated using the temperature vegetation index (TVX) space. The surface temperature was found to rise when natural land was converted into urban areas. Yuan et al. 2007 compared the performance of impervious surface area (ISA) and NDVI showing SUHI effects in the Twin Cities of Minnesota using Landsat data. A Linear Spectral Mixing Analysis (LSMA) approach was used for the classification of the percent impervious surface area (%ISA). The relationship of LST with NDVI was found to show non-linear behaviour which was strongly affected by season. The strong linear relationship of LST with %ISA was found suggesting that ISA accounts for most of the variation in LST. Alhawiti and Mitsova (2016) studied the correlation between SUHI and land uses in the City of Fort Lauderdale, located in Broward County using Landsat 8 OLI data captured on March 23rd, April 24th, October 17th, and November 2nd, 2014. They found positive correlation between NDBI and LST whereas NDVI shows negative correlation with NDBI and LST. They classified the LST map in three temperature regions and percentage of each class in these regions were determined. The results suggested that the commercial and the residential areas showed highest LST during all the four study periods. Land areas associated with transportation and utilities follow the trend close to that exhibited by commercial lands. The lower LST values were associated with the coastal wetland vegetation, followed by upland hardwood forests, rivers and lakes. Zhang and Wang 2008 studied the relation of spatial extent of SUHI with urban characteristics using Landsat 7 ETM+ data for different cities in China at almost same latitude extent. The size of urban extent, water proportion, development area, urban mean NDVI value and population density was used as urban characteristics. Hot Island area (HIA) was estimated from LST map. Relation of HIA with the urban characteristics were determined. HIA shows positive linear

correlation with urban size, development area and population density but shows negative linear correlation with water proportion and urban NDVI mean value. Hung et al. 2006 studied the effect of SUHI in Asian Mega cities (temperate and tropical climate regions) using Landsat ETM+ and MODIS day and night time data. Spatial patterns of SUHIs were examined for each city for diurnal and seasonal variations using Gaussian approximation. The SUHI effect during day time was found with higher magnitude in summer than in winter season in temperate region but the SUHI effect during day time was almost same in both the summer and winter season in tropical region. SUHI was also compared with population and was found that the magnitude of the day time SUHI is highly proportional to population size than the night time SUHI. SUHI footprint was also found to increase with population but this increase was found greater in day time than night time. Sidiqui et al. 2016 studied the SUHI effect in Sydney, Australia using MODIS data and Landsat 8 data. SUHI was determined using a Gaussian approximation method. Sydney is in temperate climate and it faces SUHI magnitudes higher in urban areas than in rural settings, particularly throughout the year, but these are most significant during summer months. Higher SUHI intensity occurred during day time in summer season whereas night time intensity values were relatively lower than day time and even dropped close to zero or negative in winter. Mukherjee et al. (2014) compared the performance of five different regression techniques for thermal sharpening of MODIS and Landsat images using Tsharp, Tsharp with local variant, Disaggregation of Radiometric Temperature (Distrad), Least Median Square Regression (LMSR) and Pace regression. The relation of LST with NDVI was used for the study over a study region in India with heterogeneity in land cover. These models were found applicable for agricultural or vegetated landscapes but not suitable for waterbodies or sandy areas. Eswar et al. (2016) used Distrad method for downscaling MODIS thermal images of different locations in India using five different indices NDVI, Fractional vegetation cover (FVC), NDWI, Soil Adjusted Vegetation

Index (SAVI) and Modified Soil Adjusted Vegetation Index (MSAVI) from 960 m to 120 m spatial resolution. NDVI/FVC showed better disaggregation result in wet areas and NDWI performed better in dry areas. Yang et al. (2017) downscaled the aggregated Landsat 8 thermal image of Nanjing city at 360 m to 90 m spatial resolution using multiple linear regression models and compared with the original Landsat LST. The LST relation with multiple scale factors with adaptive thresholds were utilized in the region with mixed land covers. The disaggregated LST image showed good result with Root Mean Square Error (RMSE) of 1.13 K and coefficient of determination of 0.87. Shirani-bidabadi et al. 2019 determined different thermal levels from the LST image to study the impact of urbanisation on LST from the years 1999 to 2016 using Landsat 7 and Landsat 8 satellite images of Isfahan city in Iran. The heat island ratio index was developed using the area within each thermal levels and studied for years i.e. 1999, 2006, 2013 and 2016. The value of the developed index increased from 1999 to 2016 due to urbanisation effect. Qi et al. 2016 developed Geographical Statistical Model (GSM) for LST sharpening using raster layers of many variables involved in land surface energy budget and thermal infrared electromagnetic radiation transmission. This study was conducted in mountain areas and found good accuracy. This method was found applicable for agriculture and forestry locations. Gao et al. 2012 developed a new Data Mining sharpener (DMS) technique for thermal sharpening and compared its performance with Tsharp method. The DMS approach builds regression trees between TIR band brightness temperatures and shortwave spectral reflectances based on intrinsic sample characteristics. The study was performed in rainfed agricultural area, irrigated agricultural region and heterogeneous naturally vegetated landscape and this method performed better in all the areas. Saavedra et al. 2017 proposed a new thermal sharpening method called TS2uRF for thermal sharpening of the Landsat 8 TIR (100 m) imagery to their visible spatial resolution (30 m). The potential of superpixels (SP) combined with regression

random forest (RRF) have been used and found improved result than Tsharp method and applicable for agricultural areas. Wang et al. used Global Regression method for thermal sharpening using different physical and statistical approach in a city whereas here, a statistical approach has been used and compared in four different cities such that the obtained thermal sharpening approach are applicable for varied cities.

The sensitivity of different SI for disaggregation of MODIS thermal image have been studied in agricultural region. The downscaling approach found useful for agricultural areas may not be suitable for urban regions. The natural land cover surrounding the urban regions may vary for different cities which can influence the result of thermal sharpening. Previous studies on thermal sharpening in urban areas may be suitable for particular cities but not for other cities having different natural surroundings. Thus, it is important to determine downscaling method that should be suitable for most of the urban regions. The relation of LST with different SI were studied and development of relations using SI in combined form have also been carried out which shows improved relation with LST. These studies have been performed for day time but the relations may vary for night time. It is important to analyse the LST relation with different SI both during day and night time to understand the thermal behaviour. Various reasearchers have also studied the integrated effect of built-ups and bare land in formation of SUHIs. The urbanisation replaces barren or vegetated areas with built-ups. In order to understand the change in SUHI effect with urbanisation, it is important to analyse the independent contribution of built-up land cover on SUHI formation.

1.15 MOTIVATION OF THE STUDY

LST has the capability to control the biological, chemical and physical processes that occurs on Earth and acts as an important parameter for the exploration of urban climate. Urbanisation has increased significantly in the last few decades, resulting in major land cover

changes in urban areas. This shows substantial impact on the LST of that region which shows adverse effect on the ambient habitat of our ecosystem. The spatial and temporal variations in SUHI formation depend on several factors that includes ISA, landscape structure, climate, vegetation cover and albedo. The variation in LST is observed with change in both space and time. The knowledge of LST dynamics with space and time is required to develop understanding about the interactions of human activities with the environment.

Satellites with thermal sensors provides LST images at different spatial and temporal resolution useful to study about the spatial and dynamic variation in LST. The fine spatial resolution LST images are limited with low temporal resolution whereas high temporal resolution LST images has low spatial resolution. The thermal images at fine spatial resolution is required for various urban applications due to greater heterogeneity in land covers in urban areas. The increment in the demand of LST images at fine spatial resolution has motivated for developing thermal sharpening methods useful for urban areas. The information content can be enhanced in the disaggregated LST images at fine spatial resolution as compared to the original coarse LST image which can be useful for various applications.

The behaviour of LST varies for different land covers with changing time of a day which results in variation of SUHI effect for day and night time. Various researchers have established the relation of LST with different SI in order to explain the behaviour of LST for different land covers. Hence, the comparison of the relation of LST with different SI is important for both day as well as night time to establish the relation required to describe the variation in LST with varying land covers.

India is the second most populous country in the world. The higher population is the major reason for the increasing urbanization in the country. The increase in urbanization

results in expansion of the city which shows significant effect on the LST pattern within the city. Therefore, there is an acute requirement to study about the SUHI growth with urban expansion. The city not only expands with increased built-ups in the outskirts of the city but the density of artificial built-ups also increases within the city. The city expansion and the increase in urban density can effect the SUHI intensity (SUHII). The neighbouring rural land covers also contributes to SUHI intensity. Thus, it is important to study the variation in SUHII for urban land covers with different kind of natural surroundings. This can be useful to understand the behavior of SUHII with increased urbanization and changing seasons.

1.16 RESEARCH OBJECTIVES

The research work performed and presented in this thesis focuses on establishing the relation of LST with various SI which can improve the explaination of LST behaviour with different land covers in urban areas and also, the study on increase in SUHI effect with increased urbanisation. The specific research objectives of this thesis are as below:

1. Disaggregation of coarse spatial resolution MODIS LST using various robust regression methods in urban areas from different climatic zones.
2. Disaggregation of MODIS LST using various statistical downscaling technique in heterogeneous cities consisting of different natural surroundings.
3. A comparative analysis of day and night LST dynamics with different SI in two semi-arid cities using satellite images and development of model which can explain the variation in LST both during day and night time.
4. Quantification of Urban Heat Intensity with LULC Changes and contribution of each land cover towards SUHI effect using Landsat Satellite Data over Urban Landscapes.
5. Assessment of seasonal and long term quantification of SUHII using MODIS satellite data.

1.17 ORGANISATION OF THESIS

This thesis decribes the research work performed during the period from July 2015 to October 2020. This thesis includes new ideas developed to understand the phenomena of SUHI effect using the satellite derived LST images. This section provides a brief introduction about the chapters and the research work carried out. The thesis was organized as below:

Chapter 1 consists of introduction to the basics of thermal remote sensing, urban heat island, research background, research objectives and motivation of the study. The literature review is also done in order to provide an overview of the previous research work performed by various researchers in the field of study on LST variation in urban areas and analysis on phenomena of SUHI effect.

Chapter 2 consists of Landsat and MODIS satellite data specifications and also the information about the data provided by the satellite sensor available at different wavelength bands. The mathematical equations used for calculation of various well known SI used in the study and also, the determination of Impervious surface fraction (ISF) using Normalized Spectral mixture analysis (NSMA) approach are discussed. Further, the estimation of LST using the radiative transfer equation from Landsat 8 thermal image are also presented in this chapter.

Chapter 3 discusses about the disaggregation of MODIS LST in urban areas using different regression methods. The comparison of the performance of six different SI like EVI, NDVI, NDBI, Urban Index (UI), Normalized Difference Soil Index (NDSI) and NDWI were carried out for disaggregation of LST images using Distrad Model over four different cities of India i.e. Bikaner, Hyderabad, Vadodara and Varanasi. The index that performed best among the indices was further used for disaggregation using two robust regression techniques i.e. LMSR and Bi-square regression. The performance of each thermal sharpening method was

investigated by measuring the RMSE and also the quality assessment of the disaggregated LST image was carried out

Chapter 4 discusses about the thermal sharpening of MODIS LST using statistical downscaling technique in four urban regions of India i.e. Bikaner, Hyderabad, Vadodara and Varanasi. Here, the performance of nine different SI were compared and various regression techniques were established using combination of SI for thermal sharpening. The best combination of indices were reported for the four cities. The ratio of RMSE to SD was calculated to evaluate the performance of the established relation for the four study sites.

Chapter 5 discusses about the LST behaviour for day and night time of different land covers in two semi-arid cities i.e. Ahmedabad and Gandhinagar. The relation of LST with three independent variables i.e. NDVI, NDBI and ISF were established for both day and night time using Landsat 8 satellite images. The relation of LST with SI were used to establish relations using the combination of SI to improve the correlation of day and night LST with the land cover. The relation established was also evaluated using MODIS images for three different seasons i.e. summer, post-monsoon and winter seasons to check the performance of the developed model with changing land covers.

Chapter 6 discusses about the variation in LST with land cover changes in Varanasi city of India from 1989 to 2018 using Landsat satellite images. A new index namely Urban Heat Intensity Ratio Index (UHIRI) was proposed to quantify the urban heat intensity in years 1989, 1997, 2008 and 2018. Further, mean LST of each land cover i.e. water, vegetation, bare land and urban was determined for images of different years used in the study and quantitative contribution of each land cover towards SUHI was determined using Land Cover Contribution Index (LCCI).

Chapter 7 discusses about the determination of SUHII for the monitoring of SUHI growth with increased urbanization. The quantification of SUHI intensity was performed for winter, summer and post-monsoon seasons for the years 2001, 2007, 2013 and 2019 in Varanasi city, India using urban heat index (UHI) obtained from the MODIS LST images. The two parameters i.e. area and the mean UHI value of the region showing SUHI effect were determined. Then, combining the two parameters, quantitative analysis of SUHII was performed for three seasons.

Chapter 8 provides the overall conclusion of the research work performed and the future work plan.